

Drawing of sprayed poly(vinyl alcohol) films

Chang Seoul* and Souk-II Mah

Department of Textile Engineering, Inha University, Incheon 405-751, Korea

(Received 28 August 1996; revised 20 November 1996)

By spraying PVA aqueous solutions, precursor films were prepared. The spray-dried PVA films have higher drawability than solution-cast PVA films. This phenomenon comes from the structure of the sprayed PVA film. The sprayed PVA films are comprised of stacked polymer particles which coalesce during drying. The ease of H-bond formation between precipitated particles made the precursor film tough. During drawing the structure changed to a fibrillar structure. The modulus and strength of the drawn sprayed PVA films are about half of those of the drawn solution-cast PVA films. © 1997 Elsevier Science Ltd.

(Keywords: poly(vinyl alcohol); sprayed films; drawing)

INTRODUCTION

Spray application of polymer solution could be a useful method in preparing polymer films. In the previous paper¹ the structure and properties of the sprayed poly(vinyl alcohol) (PVA) films were reported. The sprayed film obtained from 1 wt% aqueous PVA solution was composed of solution precipitates (size of $\sim 0.2 \mu\text{m}$). With increasing polymer concentration, the droplet or mist size increased and the spray-dried film prepared from 5 wt% solution did not have the stacked polymer-particle structure. It had a fused continuous structure with weak inter-particle regions, an intermediate state between the 1 wt% sprayed film and 5 wt% solution-cast film.

PVA is a good candidate for obtaining high strength/high modulus fibres. It has a theoretical modulus of 250 GPa along the chain direction². Many Japanese researchers have been reporting on preparing high-modulus/high-strength PVA fibres by crosslinking wet-spinning³, drawing of high molecular-weight PVA gel films^{4,5}, gel spinning from dimethyl sulfoxide/water mixture⁶, and gel spinning from hydrochloride solution⁷. Their best modulus and strength reached 70 GPa and 2.8 GPa respectively. Cha *et al.*⁶ emphasized the high melting point of PVA (230°C) in contrast to polyethylene (PE) (130°C).

On the other hand there was a report⁸ that when syndiotacticity-rich poly(vinyl pivalate) was saponificated under high shear condition, long thin fibres were produced spontaneously through self-assembly mechanism. This seems to be a simple fibre producing process, direct fibrillation during saponification.

The sprayed PVA films were tough enough to show high drawability. The drawing behaviour of the sprayed film is reported in this paper in comparison with that of the solution-cast films.

EXPERIMENTAL

Preparation of the sprayed PVA films and solution-cast films

PVA powder was purchased from Polysciences Inc.

The weight average molecular weight of the PVA was $133\,000 \text{ g mol}^{-1}$. The average degree of polymerization was estimated as 1500. The degree of saponification was over 99.5 mol%. The PVA aqueous solution was prepared by dissolving the PVA powder at 105°C for 3 h.

The same amount of methanol was mixed into the aqueous solution to promote evaporation of the solvent at the time of spray application. The substrate was heated to 60°C. We could change the thickness of the sprayed film by changing the spraying duration. The films were strong enough to be handled by hand. The details of the spraying process were described in the previous paper¹.

The solution-cast films were formed by pouring the aqueous solution on to the stainless plate and subsequent drying at room temperature for 3 weeks.

Drawing and tensile tests

Films were peeled off from the substrates. Drawing of the PVA films were conducted with an Instron type machine with a rate of 5 mm min^{-1} . The drawing temperatures were controlled by controlling the ambient air temperature in a hot chamber.

The stress-strain curves for the drawn PVA were obtained with a crosshead speed of 5 mm min^{-1} , a gauge length of 20 mm at 25°C, and a relative humidity of 60%.

Scanning electron microscopy

The surface of the PVA films was examined with a SEM (Hitachi microscope S450) after gold coating.

Birefringence

Birefringence was measured using a Nikon polarizing microscope with compensators.

Differential scanning calorimetry

The thermal behaviour was obtained by d.s.c. (Shimadzu TA-50). The heating rate of the sample was $10^\circ\text{C min}^{-1}$ throughout the experiment.

Fourier transform infrared spectroscopy

The FT*i.r.* spectra of the sprayed and solution-cast PVA films were recorded on a Nicolet 520 FT*i.r.*

* To whom correspondence should be addressed

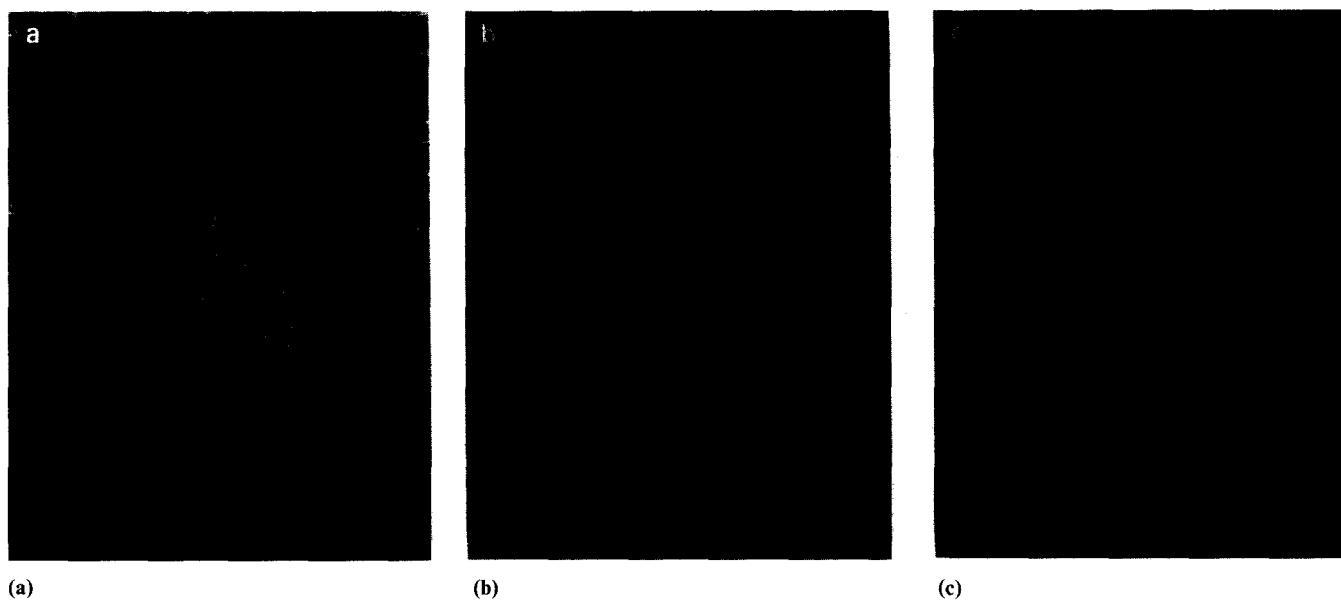


Figure 1 SEM microphotographs of (a) 1 wt% sprayed PVA film, (b) 5 wt% sprayed PVA film, and (c) 5 wt% solution-cast PVA film

spectrometer in the $4000\text{--}500\text{ cm}^{-1}$ range. Fast Fourier transforms were conducted after 32 scans.

RESULTS AND DISCUSSION

For effective film formation, aqueous PVA solutions with high polymer concentrations were forced to be sprayed by the conventional spraying equipment. Aqueous solutions with less than 5 wt% polymer concentration were sprayed successfully. The solution with a high polymer concentration over 5 wt% was too thick to be sprayed. As stated in the previous paper, the 1 wt% aqueous solution was in the dilute regime and the 5 wt% solution was in the concentrated regime.

The structure of the sprayed films was revealed by the SEM photographs shown in Figure 1. The 1 wt% sprayed film is composed of particles, the precipitate aggregates formed from the spray droplets as in Figure 1a. The 5 wt% solution-cast film has a homogeneous and coherent structure (Figure 1c). The 5 wt% sprayed film is shown in Figure 1b and has an intermediate state between the 1 wt% sprayed film and 5 wt% solution-cast film. The photograph shows artifact, micro cracks. The micro cracks were formed during electron beam irradiation and are indicative of the weaker regions in the sample. The polymer-particle structure of the 1 wt% sprayed film changes to a structure comprising a continuous phase in the 5 wt% sprayed film.

These films were tough enough to be drawn at room temperature. The maximum draw ratio of the 5 wt% sprayed PVA film increases with the increase of the drawing temperature, as shown in Figure 2. The maximum draw ratio curve is similar to that of dried PVA gel films. The sprayed film has higher maximum draw ratios than the solution-cast film. As was seen in Figure 1, the stacked-polymer-particle structure of the sprayed PVA film changed into a fibrillar structure during drawing, which was confirmed by observing the drawn sprayed films on the polarizing microscope. The H-bonds formed after the spray-drying made the films tough enough to sustain the drawing forces. The main difference in the structure of the sprayed and solution-cast film is in the structural homogeneity. The H-bond distribution of the solution-cast film is more uniform

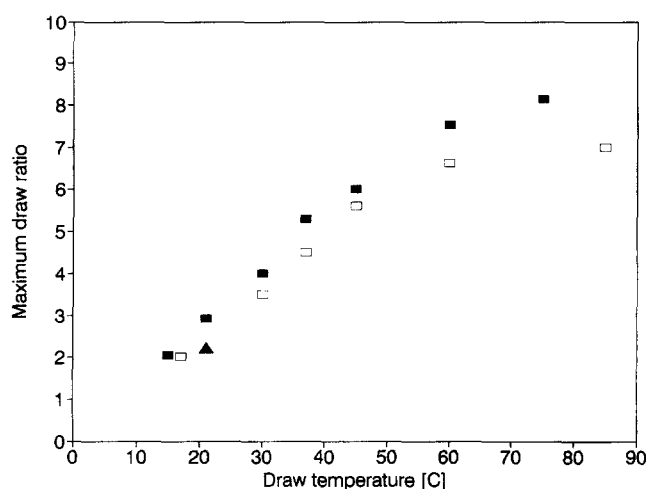


Figure 2 The relationship between the maximum draw ratio and the draw temperature for the 5 wt% sprayed PVA films (□), 5 wt% solution-cast PVA films (■) and 1 wt% sprayed PVA film (▲)

than that of the sprayed film which has relatively low H-bond density at inter-particle regions.

The sprayed films were made of precipitate aggregates, whose size must be determined from the spray mist or droplet size. After drying, the droplets solidify into solid particles and the particles coalesce (merge) into a coherent film. As the coalesced particles are connected through the newly formed H-bonds between different polymer particles, the H-bond density of the sprayed film is lower than that of the solution-cast film, especially in the inter-particle regions. The high drawability of the sprayed film means that local drawing prevails at inter-particle regions. The sprayed film from 1 wt% solution was somewhat brittle and less drawable.

In Figure 3, the dependence of birefringence on the draw ratio of sprayed and solution-cast films are shown. Birefringence increases with increasing draw ratio of the PVA films. The intrinsic birefringence values of the crystalline and amorphous phase were estimated as 51.8×10^{-3} and 43.8×10^{-3} , respectively^{9,10}. Both of the sample films have relatively low chain orientation compared to that of the coextruded PVA films. Shibayama *et al.*¹⁰ reported that the solid-state coextruded PVA film

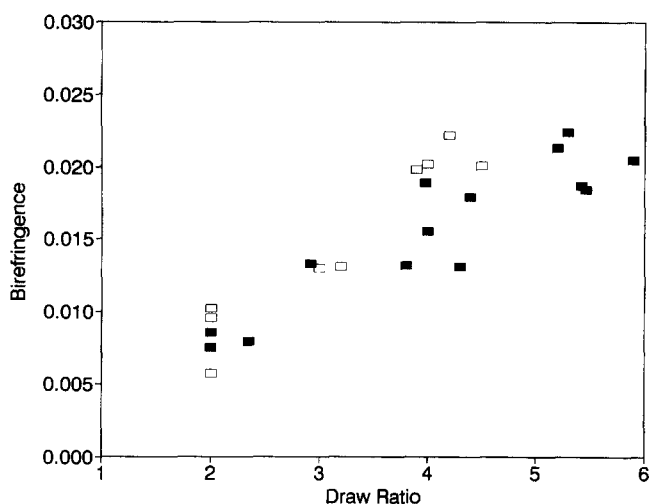


Figure 3 The dependence of birefringence on the draw ratio for the 5 wt% sprayed PVA films (\square) and 5 wt% solution-cast PVA films (\blacksquare)

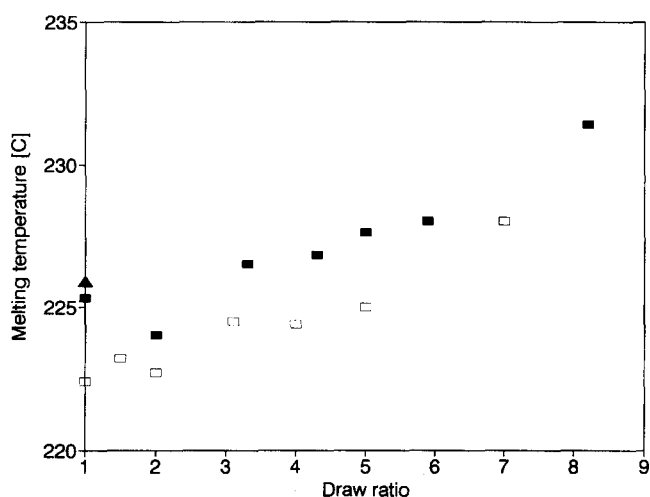


Figure 4 The dependence of peak melting temperature on the draw ratio for the 5 wt% sprayed PVA films (\square), 5 wt% solution-cast PVA films (\blacksquare) and 1 wt% sprayed PVA film (\blacktriangle)

followed the affine deformation behaviour up to a molecular draw ratio of *ca.* 5. They emphasized the positive effect of hydrogen bonding on extension. Birefringence of the solution-cast film was higher than that of the sprayed films. This stands for the effectiveness of the homogeneous drawing for the solution-cast film.

The d.s.c. heating curves of the drawn PVA films are similar to that of undrawn PVA films except shifting in the melting temperature. Figures 4 and 5 represent the dependence of peak melting temperature and heat of fusion on the draw ratio for the sprayed and solution-cast films, respectively. Both the peak melting point temperature and heat of fusion also increase as the draw ratio increases for both of the films. The peak melting point and heat of fusion of the sprayed films are higher than those of the solution-cast film at all draw ratio range. Undrawn sprayed PVA film had higher melting point and heat of fusion than those of the solution-cast film. The crystallinity of the drawn PVA film was calculated from the endothermic melting peak area. The 100% perfect PVA crystal was assumed to be 156 J g^{-1} . The crystallinity of the sprayed film changed from 0.38 to 0.45 for the sample with a draw ratio of 8.

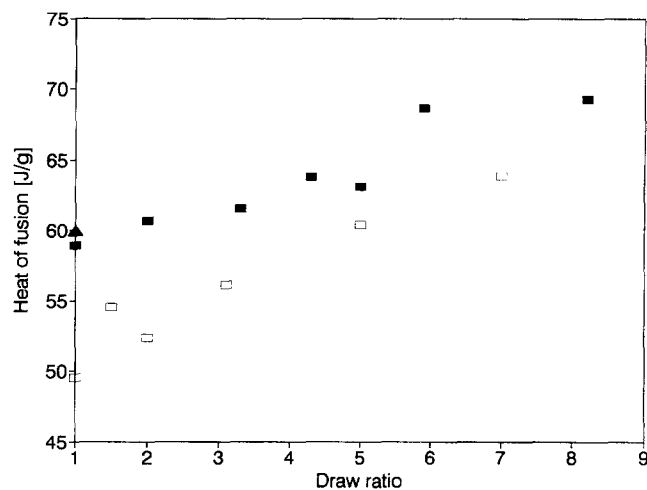


Figure 5 The dependence of the heat of fusion on the draw ratio for the 5 wt% sprayed PVA films (\square), 5 wt% solution-cast PVA films (\blacksquare) and 1 wt% sprayed PVA film (\blacktriangle)

The sprayed films had higher crystallinity than the solution-cast film at all draw ratios. Drawing process accompanies the structural change from the stacked polymer particle structure into the fibrillar structure. Chains in the inter-particle regions are interconnected through the newly formed H-bonds. Deformation occurs mainly in the inter-particle regions. Occurrence of the local drawing behaviour at inter-particle regions left most of the crystalline regions untouched for the sprayed film. The solution-cast film exhibits large structure destruction at low draw ratios. With increasing the draw ratio the molecular chains rearrange into a fibrillar structure. The H-bonding in PVA films prevents slippage of chains on deformation and effectively transfers the external drawing stress/strain to the molecular level. The ease of H-bond formation in PVA film is the key factor for the high drawability of the sprayed PVA films. Thus if we prepared sprayed films of H-bond forming polymers from really fine particles, i.e. single molecule particles¹¹, we can achieve a high draw ratio for this kind of polymer. It is H-bondings formed during drying between fine polymer particles that make the sprayed film more drawable.

In Figure 6 FTi.r. spectra obtained with a polarizer for the 5 \times drawn sprayed PVA films are shown. The small H_2O bands and CO_2 band at 660 cm^{-1} are due to the material in the i.r. sample chamber. The spectra have absorption bands at 850, 923, 1026, 1104, 1140, 1243, 1334, 1430, 1570, 1670, 2900, 2930 and a broad band at $3500\text{--}3100 \text{ cm}^{-1}$. Similar spectra were obtained for the sample with polarized i.r. beam along and perpendicular to the stretching direction.

The distinct differences are found on the band at 1144 cm^{-1} . Usually this absorption band has been proposed for the estimation of the degree of crystallinity in PVA¹¹. From these spectra, we could assign each band's direction of the transition moment. The absorption band at 850, 923, 1140, 1334 cm^{-1} weakened in their intensity, which means the transition moment oriented perpendicular to the stretching direction. The absorption band at 1243 cm^{-1} has a transition moment along the fibre axis.

The absorption at 650 cm^{-1} arises from C-C-C stretching, 918 -OH, 1100 secondary alcohol, 1240 CH_2 -twisting, 1330 -OH bending, and 1430 CH_2 -twisting.

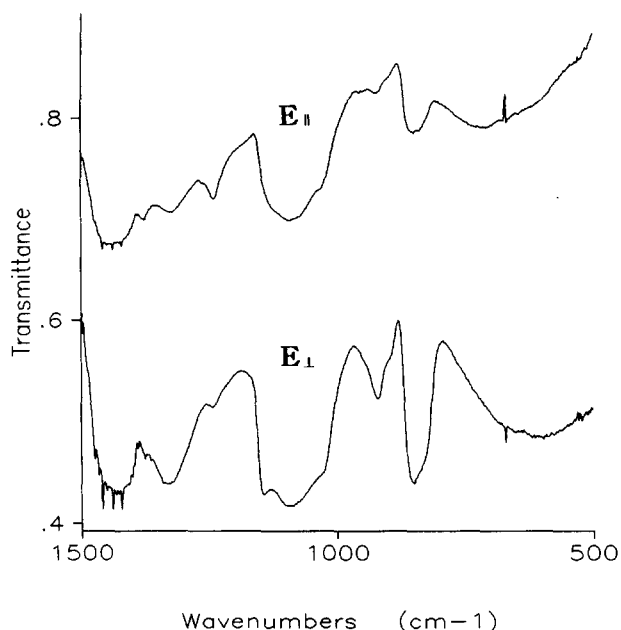


Figure 6 FTIR spectra for a 5x drawn PVA sprayed film measured with the polarized i.r. beam whose electric vector parallel ($E_{||}$) and perpendicular (E_{\perp}) to the fibre axis

The OH-bending bands at 920 and 1330 cm^{-1} strengthen as the polarized incident i.r. beam directs along the perpendicular to the fibre axis. Thus the absorption band at 1144 cm^{-1} seems to represent for the degree of H-bonding arising from the OH groups in the crystalline region.

When polarized i.r. radiation is used with samples oriented by stretching, the intensity of most of the bands increases when the plane of polarization is perpendicular to the direction of stretching, but a few bands show parallel dichroism. The bands at 640, 1087, 1235 and 1440 cm^{-1} have transition moments along the polymer chain and the bands at 850, 916, 1040, 1096, 1144 and 1326 cm^{-1} have transition moments perpendicular to the polymer chain. We can confirm this rule in Figure 6.

According to Krimm *et al.*¹², the band at 1144 arises from C–O of doubly hydrogen-bonded OH in crystalline regions and the band at 1096 corresponds to unbonded C–O in the amorphous regions. For the 5x drawn sprayed PVA film, the dichroic ratio at 1144 cm^{-1} $A_{||}/A_{\perp} = 1.23$.

Figures 7 and 8 show the draw ratio dependences of the tensile modulus and strength of the 5 wt% sprayed and solution-cast films respectively. Both tensile modulus and strength increase with draw ratio. The tensile modulus and strength of a 8x drawn sprayed film were 8.2 GPa and 0.48 GPa respectively. These values are near to the result of the drawn PVA gel films. This result proves the effectiveness of drawing of the sprayed PVA films. The H-bonds formed during drying for the sprayed PVA films makes the sample more drawable than solution-cast films.

CONCLUSIONS

The sprayed PVA films were tough enough to sustain further drawing. The maximum draw ratio of the sprayed films was slightly higher than that of solution-cast films.

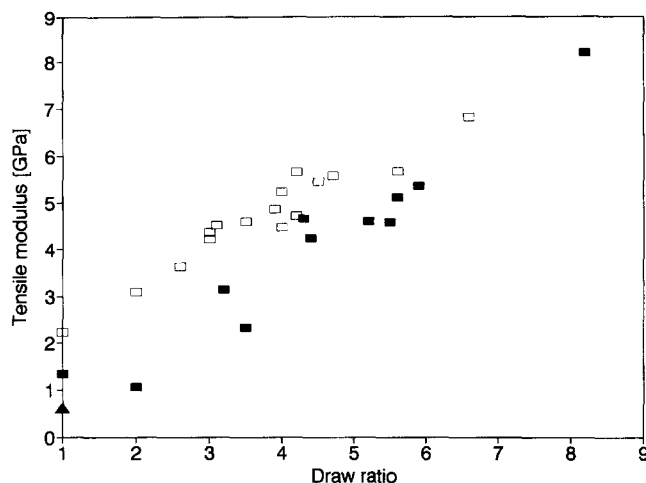


Figure 7 Tensile modulus vs. draw ratio for the 5 wt% sprayed PVA films (□), the 5 wt% solution-cast PVA films (■) and 1 wt% sprayed PVA film (▲)

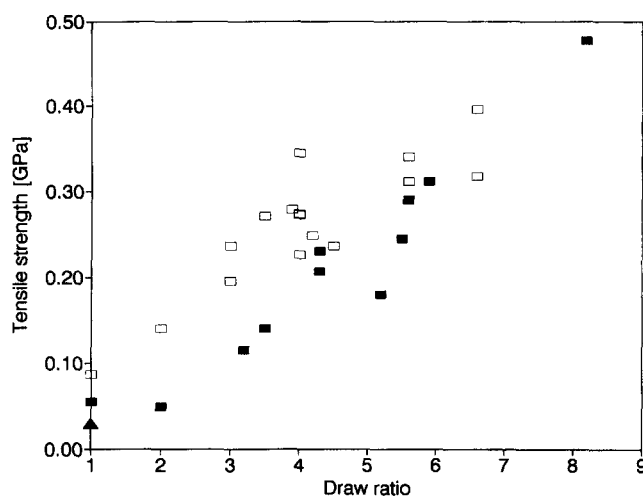


Figure 8 Tensile strength vs draw ratio for the 5 wt% sprayed PVA films (□), the solution-cast PVA films (■) and 1 wt% sprayed PVA film (▲)

The sprayed PVA films prepared from 1 wt% solution comprise stacked polymer particles. The sprayed film prepared from 5 wt% solution has a continuous structure with weak inter-particle regions. Upon drawing the sprayed film, the deformation behaviour was similar to that of dried PVA gel films. The drawn sprayed PVA film had all the special features that the highly drawn polymer had, e.g. high chain orientation, increase in birefringence, heat of fusion, initial modulus, and strength with the increase of draw ratio. The high drawability of the sprayed PVA film originates from the relatively low H-bond density at inter-particle regions. The easy H-bond formation between PVA chains leads to the high drawability.

The tensile modulus and strength of a 8x drawn sprayed film were 8.2 GPa and 0.48 GPa, respectively. These values are comparable to those of PVA gel films or gel-spun fibres, if we take into consideration the effect of the molecular weight of the sample.

Although the drawability of the sprayed PVA film was improved a little, we found a new method to produce strong PVA films.

ACKNOWLEDGEMENT

This work was supported by the 1995 year program of the Inha University research funding.

REFERENCES

1. Seoul, C., *J. Kor. Fiber Soc.*, 1995, **32**(7), 654.
2. Sakurada, I., Ito, T. and Nakamae, K., *J. Polym. Sci. (C)*, 1966, **15**, 75.
3. Fujiwara, H., Shibayama, M., Chen, J. H. and Nomura, S., *J. Appl. Polym. Sci.*, 1989, **37**, 1403.
4. Hong, P. D. and Miyasaka, K., *Polymer*, 1991, **32**, 3140.
5. Kobayashi, M. and Kanamoto, T., *Proc. ISF '94*. Yakohama, Japan, 1994, p. 339.
6. Cha, W.-I., Hyon, S.-H. and Ikada, Y., *J. Polym. Sci., Polym. Phys.*, 1994, **32**, 297.
7. Okazaki, M., Miyasaka, Y. and Matsuzawa, S., *Kobunshi Ronbunshu*, 1995, **52**(11), 710.
8. Riu, W. S., Ph.D. Dissertation, Seoul National University, 1994.
9. Hibi, S., Maeda, M. and Takeuchi, M., *Sen-i Gakkaishi*, 1971, **27**(2), 41.
10. Shibayama, M., Kurokawa, H., Nomura, S., Roy, S., Stein, R. S. and Wu, W., *Macromolecules*, 1990, **23**, 1438.
11. Bu, H., Chen, E., Xu, S., Guo, K. and Wunderlich, B., *J. Polym. Sci., Polym. Phys.*, 1994, **32**, 1351.
12. Siesler, H. W. and Holland-Moritz, K., *Infrared and Raman Spectroscopy of Polymers*. Marcel Dekker, New York, 1980, p. 70.
13. Krimm, S., Liang, C. Y. and Sutherland, G. B. B. M., *J. Polym. Sci.*, 1956, **22**, 227.